Earth Syst. Sci. Data, 15, 4163–4179, 2023
https://doi.org/10.5194/essd-15-4163-2023


Open Access Earth System Science Data

# Bio-optical properties of the cyanobacterium *Nodularia spumigena*

**Shungudzemwoyo P. Garaba[1], Michelle Albinus[1], Guido Bonthond[2], Sabine Flöder[3], Mario L. M. Miranda[4,5], Sven Rohde[2], Joanne Y. L. Yong[3], and Jochen Wollschläger[1]**

[1]Marine Sensor Systems Group, Center for Marine Sensors, Institute for Chemistry and Biology of the Marine Environment, Carl von Ossietzky University of Oldenburg, Schleusenstraße 1, 26382 Wilhelmshaven, Germany
[2]Environmental Biochemistry Group, Institute for Chemistry and Biology of the Marine Environment, Carl von Ossietzky University of Oldenburg, Schleusenstraße 1, 26382 Wilhelmshaven, Germany
[3]Plankton Ecology Group, Institute for Chemistry and Biology of the Marine Environment, Carl von Ossietzky University of Oldenburg, Schleusenstraße 1, 26382 Wilhelmshaven, Germany
[4]Laboratorio de la Calidad del Agua y Aire, Universidad de Panamá, P.O. Box 0824, Panama City, Panama
[5]Sistema Nacional de Investigación, Secretaría Nacional de Ciencia y Tecnologías, P.O. Box 0816-02852, Panama City, Panama

**Correspondence:** Shungudzemwoyo P. Garaba (shungu.garaba@uni-oldenburg.de)

Received: 16 January 2023 – Discussion started: 26 January 2023
Revised: 11 August 2023 – Accepted: 16 August 2023 – Published: 22 September 2023

**Abstract.** In the last century, an increasing number of extreme weather events have been experienced across the globe. These events have also been linked to changes in water quality, especially due to heavy rains, flooding, or droughts. In terms of blue economic activities, harmful algal bloom events can pose a major threat, especially when they become widespread and last for several days. We present and discuss advanced measurements of a bloom dominated by the cyanobacterium *Nodularia spumigena* conducted by hyperspectral optical technologies via experiments of opportunity. Absorption coefficients, absorbance and fluorescence were measured in the laboratory, and these data are available at https://doi.org/10.4121/21610995.v1 (Wollschläger et al., 2022), https://doi.org/10.4121/21822051.v1 (Miranda et al., 2023) and https://doi.org/10.4121/21904632.v1 (Miranda and Garaba, 2023). Data used to derive the above-water reflectance are available from https://doi.org/10.4121/21814977.v1 (Garaba, 2023) and https://doi.org/10.4121/21814773.v1 (Garaba and Albinus, 2023). Additionally, hyperspectral fluorescence measurements of the dissolved compounds in the water were carried out. These hyperspectral measurements were conducted over a wide spectrum (200–2500 nm). Diagnostic optical features were determined using robust statistical techniques. Water clarity was inferred from Secchi disc measurements (https://doi.org/10.1594/PANGAEA.951239, Garaba and Albinus, 2022). Identification of the cyanobacterium was completed via visual analysis under a microscope. Full sequences of the 16S rRNA and rbcL genes were obtained, revealing a very strong match to *N. spumigena*; these data are available via GenBank: https://www.ncbi.nlm.nih.gov/nuccore/OP918142/ (Garaba and Bonthond, 2022b) and https://www.ncbi.nlm.nih.gov/nuccore/OP925098 (Garaba and Bonthond, 2022a). The chlorophyll-*a* and phycocyanin levels determined are available from https://doi.org/10.4121/21792665.v1 (Rohde et al., 2023). Our experiments of opportunity echo the importance of sustainable, simplified, coordinated and continuous water quality monitoring as a way to thrive with respect to the targets set in the United Nations Sustainable Development Goals (e.g. 6, 11, 12 and 14) or the European Union Framework Directives (e.g. the Water Framework Directive and Marine Strategy Framework Directive).

Published by Copernicus Publications.

## 1 Introduction

Photosynthetic eukaryotic microalgae as well as cyanobacteria play an important role as primary producers in aquatic ecosystems. These primary producers form the basis of the aquatic food web, fix carbon, produce oxygen and are involved in nutrient cycling. However, when certain environmental variables favour the excessive growth and accumulation of any particular species, it becomes an algal bloom. Such an event becomes detrimental (i.e. a harmful algal bloom, HAB) when the bloom-forming species produce toxins or have a negative impact on other aquatic organisms due to their inherent sheer biomass in the water (Karlson et al., 2021; Smayda, 1997; Carmichael, 1992; Francis, 1878). Some of the HABs can have damaging effects on socioeconomic factors, including human health; animals; aquaculture; and the recreation, fishing and tourism industries (Glibert et al., 2005; Hallegraeff et al., 2003; IOCCG, 2021; Mazur and Pliński, 2003; Karlson et al., 2021; Nehring, 1993).

Cyanobacteria are known to cause cyanobacterial HABs (cyanoHABs) in fresh to brackish waters, which often manifest as unsightly scum that accumulates on the surface and shores of waterbodies. An example is the cyanobacterium *Nodularia spumigena* (hereafter *N. spumigena*) found in soil and diverse geographic aquatic environments (Horstmann, 1975; Kahru et al., 1994; Öström, 1976; Mazur and Pliński, 2003; Karlsson et al., 2005; da Silveira et al., 2017). *N. spumigena* is a diazotrophic filamentous cyanobacteria that can form blooms during the Northern Hemisphere summer, during which time water temperatures rise above $\sim 16\,^{\circ}\mathrm{C}$ in a calm weather state with long hours of direct ambient light (Lehtimaki et al., 1997; Wasmund, 1997; Kanoshina et al., 2003; Olofsson et al., 2020). These environmental conditions result in the stratification of the water column and a nutrient depletion that is conducive to the growth of heterocystous filamentous cyanobacteria species such as *N. spumigena* in the euphotic zone (Karlberg and Wulff, 2013). An increasing number of cyanoHABs are expected in the wake of climate change, with extreme weather events producing favourable environmental conditions for blooms (Chapra et al., 2017). Consequently, a rise in the demand for near-real-time monitoring strategies, such as remote sensing capable of offering wide-area and repeated coverage of all aquatic environments at varying geospatial resolutions, is expected.

Wide-area, repeated monitoring of *N. spumigena* has been achieved in the Baltic Sea and other geographic locations using multispectral satellite missions in the last few decades (Kahru et al., 1994; Öström, 1976; Kahru and Elmgren, 2014; Galat et al., 1990; Leppänen et al., 1995; Mazur and Pliński, 2003). As some reports have revealed, there are *N. spumigena* strains that can be very harmful and toxic to animals or humans, further stressing the importance of the detection and identification of such related blooms (e.g. Teikari et al., 2018; Nehring, 1993; Sivonen et al., 1989). Furthermore, recent advances in remote-sensing technologies have also resulted in a rising number of laboratory-based hyperspectral investigations of HABs to better understand and identify inherent diagnostic spectral features of various algae, e.g. *N. spumigena* (Soja-Woźniak et al., 2018). A gap in interdisciplinary datasets as well as diverse hyperspectral measurements has been echoed in recent scientific user needs discussion and research studies focussed on future satellite missions relevant for monitoring the aquatic environment (e.g. IOCCG, 2021; Bracher et al., 2017; Hu et al., 2022; Castagna et al., 2022). To this end, we report on experiments of opportunity in which a set of hyperspectral observations were conducted following *N. spumigena* bloom events in an enclosed waterbody, Lake Bante in Wilhelmshaven, Germany. These high-quality observations are expected to expand the diversity in open-access spectral reference libraries of hyperspectral inherent and apparent bio-optical measurements that will contribute towards future algorithm development, validation and identification of diagnostic spectral features of blooms resulting from *N. spumigena*.

## 2 Methods and materials

### 2.1 Field campaign sampling

A dark-green, dense bloom was visually observed on Lake Bante (also known as Banter See or Lake Bant) in Wilhelmshaven, Germany, on 16 August 2021 (Fig. 1). Lake Bante is a former harbour basin, now cut off from the rest of the port, that exhibits brackish to freshwater conditions and extends over $\sim 2.5\,\mathrm{km} \times 0.6\,\mathrm{km}$ with a maximum depth of 22 m. From observation and general knowledge, it is known that the apparent colour of the water in the lake is relatively light green. The area of interest is near a walking path that is frequented by locals and a variety of birds, including ducks. In this study, the absence of these ducks was one of the primary indicators that triggered a further investigation of the easily accessible part of Lake Bante, leading to our discovery of the bloom and, hence, our experiment of opportunity. Sampling was conducted using a measuring cup and two 1000 mL Schott DURAN bottles that had been pre-rinsed three times with the sample water. Samples of water from areas that could be considered representative of bloom and non-bloom conditions, respectively, were collected close to each other. We also visually distinguished these waters based on the apparent colour and density of bloom material. Laboratory measurements were conducted immediately after sampling; therefore, no storage in the fridge nor in the dark was considered necessary.

A similar bloom appeared in Lake Bante and was surveyed from 10:00 to 12:00 UTC on 25 August 2022; sampling was conducted at 14 stations from a small electric-powered boat (Fig. 1b). The water samples were collected following the

steps used in the August 2021 campaign, but additional parameters like geolocation, time, salinity and temperature information for each station were also gathered using a Xylem Inc. SonTek CastAway™ CTD (conductivity–temperature–depth) instrument. Storage of the samples was done in a fridge at 4 °C until filtration or further analysis. Calibrated data were retrieved from the CTD unit via a Bluetooth connection in the CastAway™ CTD software (version 1.5.). Water transparency was inferred from Secchi disc depth measurements. The Secchi disc had a diameter of 30 cm with four equal quadrants in alternating black and white colours.

### 2.2 Laboratory imaging

The collected August 2021 bloom water in one of the Schott DURAN bottles was made homogenous by shaking, and a sample was then taken for microscopic analysis. A 1 : 2 dilution ratio with sterile seawater was used because the collected sample was relatively thick and viscous due to the high concentration of cyanobacteria filaments. A further 1 : 30 dilution, 110 µL sample + 3190 µL sterile seawater, was completed and left to settle in a HYDRO-BIOS Apparatebau Utermöhl sedimentation chamber. The samples were examined under a Zeiss Axiovert 10 inverted microscope between 10× and 40× magnification following the method of Utermöhl (Utermöhl, 1931). Oculars with 10× magnification were used in combination with the above-mentioned microscope objectives (10× to 40×). The identification of the bloom-causing organism based on cell morphology was completed using the literature (Komárek, 2013). Photographs were taken with a JENOPTIK PROGRES® GRYPHAX® KAPELLA microscope camera. Additionally, automated imaging was completed in a Yokogawa Fluid Imaging Technologies FlowCam 8400 system. For the latter, sample preparation involved filtration through a 100 µm mesh to prevent clogging in the system, and the analysed volume of the filtrate was 2.5 mL. No further microscopic inspection was conducted for the August 2022 samples, as this had been performed for the 2021 campaign.

### 2.3 Deoxyribonucleic acid (DNA) extraction and sequencing

A molecular genetic confirmation of the bloom-causing organism was done using the samples from August 2022 to further verify the visual taxonomic identification conducted in August 2021. Water samples (10 mL) were filtered using membrane filters Whatman Nuclepore™ track-etched membranes with a 0.2 µm pore size and 47 mm diameter. The filters were frozen at −80 °C until further analysis. After cutting the filters into small fragments, DNA was extracted using a ZYMO Research D6102 fecal/soil microbe kit following the manufacturer's protocol. The 16S rRNA and rbcL genes were amplified using polymerase chain reaction (PCR) with a Thermo Scientific Phusion Green Hot Start II High-Fidelity PCR Mastermix and the universal 27F and 1492R primers (5′-AGAGTTTGATCMTGGCTCAG-3′ and 5′-GGTTACCTTGTTACGACTT-3′, respectively) for the 16S rRNA gene and the CX and CW primers (5′-GGCGCAGGTAAGAAAGGGTTTCGTA-3′ and 5′-CGTAGCTTCCGGTGGTATCCACGT-3′, respectively) for the rbcL gene. After an initial denaturation step at 98 °C for 3 min, the reaction included 30 cycles of 30 s at 98 °C, 30 s at 50 °C, and 30 s at 72 °C as well as a final step of 3 min at 72 °C. Amplicons were sequenced in forward and reverse direction at Eurofins Genomics, Germany. As the chromatograms of the 16S rRNA gene contained some background signal, cyanobacteria-specific primers were designed for the 16S rRNA gene (5'-CCTAGCTTAACTAGGTAAAAAG-3', 5'-TACAAGGCTAGAGTGCG-3' and their reversed complements), and new amplicons were generated and sequenced with the same PCR protocol and program.

### 2.4 Optical measurement and analysis

#### 2.4.1 Absorbance

Water samples from the 25 August 2022 survey were filtered through Whatman Nuclepore™ track-etched membranes with a 0.2 µm pore size and 47 mm diameter. The filters were frozen and stored at −80 °C. Each frozen filter was put into a separate 20 mL glass vial before a 5 mL aliquot of 1× phosphate-buffered saline with a pH = 7 was added to begin a pigment concentration analysis. Sample sonification was completed in an ultrasonic bath filled with crushed ice; this was carried out four times in 1 min pulses with 60 s pauses in between. After sonification, the glass vial were centrifuged and three 250 µL aliquots of the supernatant were transferred onto a 96-microwell plate. A BioTek Instruments Synergy H1 hybrid multi-mode microplate reader was used to determine the absorbance of the samples. Phycocyanin concentrations ($\mu g\,L^{-1}$) were computed as recommended in the literature (Horváth et al., 2013). The remaining supernatant was decanted, and the filters were frozen again at −22 °C. Samples were freeze-dried for a day, and 5 mL of 99.5 % ethanol was then added to each glass vial. Alcoholic extracts were prepared as explained above, and the samples were centrifuged before the supernatant from each sample was measured in the microplate reader. Chlorophyll-*a* concentrations ($mg\,L^{-1}$) were determined following the standard protocol (Ritchie, 2008).

#### 2.4.2 Absorption coefficients

Hyperspectral absorption coefficients in the visible spectrum (400–700 nm) were determined directly after sampling using a point-source integrating cavity absorption meter, PSICAM (Kirk, 1997; Röttgers and Doerffer, 2007). The PSICAM had an Illumination Technologies CF1000e halogen lamp as the

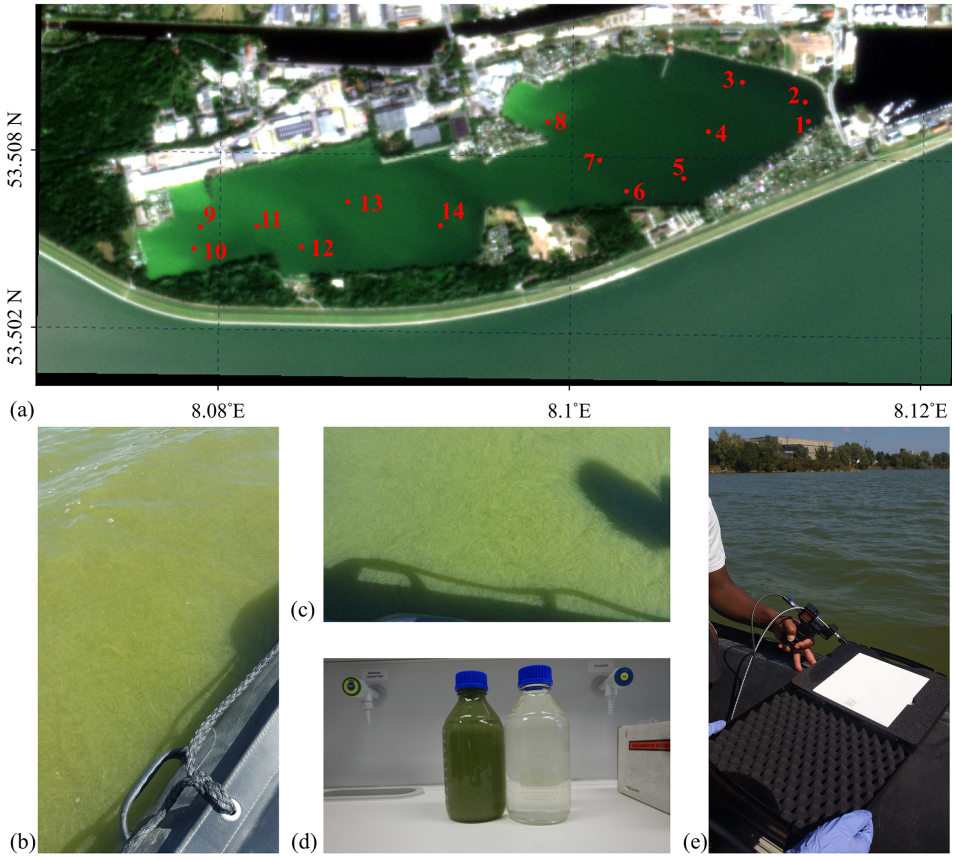


**Figure 1.** **(a)** PlanetScope SuperDove satellite 248b true-colour RGB composite image captured at 10:07 UTC on 25 August 2022 over Lake Bante in Wilhelmshaven, Germany; **(b–c)** photographs of the dense bloom as observed around station 13; **(d)** water samples from 16 August 2021 collected from 53.5093° N, 8.114° E from the shoreline close to station 1; and **(e)** radiometric measurements during the 2022 survey.

light source and used an Avantes AvaSpec ULS 2048XL-RS-EVO spectrometer as the detector. The instrument was calibrated using a solution of nigrosin with a maximum absorption coefficient of $\sim 0.5\,m^{-1}$. Sartorius Airum® Pro ultrapure water was used as a reference for both the calibration and sample measurements. For the bloom in 2021, as explained above, the bloom water was very concentrated; therefore, we diluted the sample at a ratio of 1 : 80 (Fig. 1d), and only the total absorption of the water constituents ($a_{tot}$) was measured. The samples of the 2022 campaign were analysed for both $a_{tot}$ and absorption of coloured dissolved organic material ($a_{cdom}$). For this, the samples were filtered through 0.2 µm pore size Whatman Nuclepore™ track-etched membrane filters. As the $a_{tot}$ samples were less dense than in 2021, the samples were only diluted at a ratio of 1 : 10. The $a_{cdom}$ samples remained undiluted. The absorption coefficients of the particulate fraction were obtained via the subtraction of $a_{cdom}$ from $a_{tot}$ and denoted as $a_{ph}$, assuming no relevant contribution of non-algae particles.

The absorption coefficient measurements were performed in triplicate, meaning the sample was put in and out of the PSICAM three times, and each time an absorption spectrum measurement was obtained. Each measurement was the average of 20 single readings by the spectrometer, to minimize noise in the recorded signal, which could also contribute to a smoother spectrum. Data processing of absorption spectra incorporates smoothing using loess local regression which is important in case of very low absorption coefficients. However, we compared unsmoothed and smoothed spectra, and no significant differences were found, which was expected due to the high absorption of the samples. After the measurement of the samples, the respective dilution factor used was considered in the final calculation of the absorption coefficient values.

### 2.4.3 Fluorescence and excitation–emission matrix (EEM) analysis

Bloom water was pre-filtered through Whatman 0.7 µm mesh size GF/F filters and subsequently filtered through Whatman Nuclepore™ track-etched 0.2 µm pore size membranes to remove suspended solids within 72 h of sampling on 16 August 2021. A similar approach was implemented for the August 2022 campaign, but filtration was applied within 2 weeks of field sampling. Sample filtrate from the 2021

campaign was diluted with deionized water at a ratio of 1 : 4 to avoid the inner-filter effect and detector saturation. No dilution was applied for the 2022 samples. A HORIBA Aqualog benchtop fluorometer was used to obtain excitation–emission matrices (EEMs) and absorbance measurements in a 1 cm quartz cuvette containing the sample filtrate. The cuvette had been pre-rinsed three times with the sample filtrate. Spectra were recorded at a 10 nm resolution for both excitation and emission determinations. Excitation was done at 2 nm intervals from the ultraviolet to red spectrum (200–600 nm), whereas fluorescence was measured over a wavelength range of 200 to 620 nm at 1.617 nm steps. Although emission raw data can be obtained up to 620 nm, we restrict the analyses to 600 nm. Laboratory experiments have revealed that our HORIBA Aqualog benchtop fluorometer has a relatively low signal-to-noise ratio and sensitivity beyond 600 nm. A three-dimensional dataset is generated from the emission, excitation and sample measurement.

Within the scope of this dataset description, an additional analysis was performed to highlight the added value of the obtained EEM measurements to the scientific community. Using the 2021 dataset only, the derived EEMs were corrected using the DrEEM toolbox and further analysed using PARAllel FACtor analysis, PARAFAC (Murphy et al., 2013). The PARAFAC correction removed Raman and Rayleigh scattering components from the measurements followed by a normalization to Raman units. Multivariate analysis of the three-dimensional dataset obtained from the EEMs allows for the isolation of principal components associated with specific moieties in the dissolved organic material pool. A dense algal bloom can be characterized, with caveats, by the increment in the metabolic processes responsible for the release of dissolved organic compounds such as polymers, amino acids residues and decaying cells. Therefore, PARAFAC was utilized to characterize changes in the main composition of surface waters due to fluorescent dissolved organic matter produced in situ, thereby identifying and isolating fluorescent components related to microbiological activity. Principal components were validated by a split-half analysis in the DrEEM toolbox, and a model explaining over 99.5 % of the dataset variability was fitted for the analysed samples. PARAFAC was performed using MathWorks MATLAB 2017b, as detailed in a prior report (Miranda et al., 2020). Intercomparison of measured EEMs was completed in OpenFluor (Murphy et al., 2014).

#### 2.4.4 Spectral reflectance and radiance

Laboratory-based relative hyperspectral reflectance measurements of the undiluted sample were conducted on 12 August 2021 using a Spectral Evolution (SEV) SR-3501 spectroradiometer fitted with a lens having an 8° field of view and the collected data interpolated to a 1 nm resolution from the ultraviolet (UV, 280 nm) to short-wave infrared (SWIR, 2500 nm) spectrum. Observations with the SEV were performed in reflectance mode; this involved white referencing with a 20 cm × 20 cm SphereOptics Zenith Polymer® SG3120 ≈ 99 % full-material PTFE diffuse standard to determine the relative reflectance of bloom water sample. The derived relative reflectance was automatically divided by the calibration values of the white diffuse standard supplied by the manufacturer. An ARRILITE Plus 575 W high-performance halogen lamp placed at a viewing angle of 45° and at a height of 30 cm from the sample was used as a light source in a dark calibration laboratory. No additional background corrections were done, as the sample was very dense and optically deep (Fig. 1). Furthermore, the sample had been placed in a dark container with negligible reflectance. Observations were done 5 cm above the sample at nadir, resulting in a target pixel with a diameter of 0.7 cm, and each measurement was an average of 30 scans. Additional analyses on these measurements were conducted in MathWorks MATLAB R2020b, including computing the derivative, spectral angle mapping and absorption feature identification, as proposed in previous work (Liutkus, 2015; Garaba and Dierssen, 2020; Garaba et al., 2021).

Radiance measurements that were calibrated in situ were also completed aboard a small electric-motor-powered boat on 25 August 2022 on Lake Bante. The SEV was operated in radiance mode with each observation set to be an average of 20 scans, and pseudo-replicate measurements were collected from stations 1 to 11 (Fig. 1a). Sampling at each station was performed in a series of three radiance measurements over the targets: (i) diffuse white panel $= E_d$, (ii) water surface $= L_{sfc}$ and (iii) sky $= L_{sky}$ at a $\sim 45°$ viewing angle from nadir. The diffuse white panel was the same 20 cm × 20 cm SphereOptics Zenith Polymer® SG3120 ≈ 99 % full-material PTFE diffuse standard. Efforts were made to maintain a 90–135° azimuthal angle from the sensor heading to the Sun to mitigate specular reflection (Garaba and Zielinski, 2013). A set of at least four to six pseudo-replicate observations were achieved at the survey stations, as this was dependent on the drift and rotation of the boat. The rotation of the boat sometimes resulted in non-optimal viewing geometry that meant the presence of surface-reflected glint. Spectral reflectance ($R$) was derived by assuming a flat sea surface with a $\rho = 0.021$, and the manufacturer calibration reflectance of the diffuse white panel was not applied for brevity.

$$R = \frac{L_{sfc} - \rho \cdot L_{sky}}{E_d} \quad (1)$$

The surface-reflected glint as determined from visual inspection was believed to be minimal, as the lake was relatively calm during the field campaign. However, to allow future users of the radiance observation to apply a surface-reflected glint correction of choice, the quality-controlled, calibrated radiometric quantities required (Eq. 1) were made openly available (Garaba and Albinus, 2023).

## 3 Results

### 3.1 Imaging and visual microscopic properties of the algae

The cells dominating the bloom sample in 2021 were visually identified as a member of the cyanobacteria genus *Nodularia* – that is, *N. spumigena* (Fig. 2). Filaments of *N. spumigena* are unipolar; straight or curved; and yellowish, olive-green or blue-green in colour (Guiry and Guiry, 2021). The inherent heterocysts differ in appearance and size only slightly from the vegetative cell. *N. spumigena* is known to inhabit low-salinity or brackish waters, like the Lake Bante water type, where it can form larger blooms. One of the first reported cases of harmful *N. spumigena* blooms in Lake Bante dates back to August 1990 (Nehring, 1993). Although not determined in this current study, the 1990 HAB was dense, with a 6 cm thickness, and was concentrated at the western end of the lake, due to the easterly winds typically experienced in August, with the temperature range of 15–22 °C (Nehring, 1993). Based on visual inspection, the samples of 2022 were similar to those of 2021.

### 3.2 DNA genetic identification

Full sequences were obtained of the 16S rRNA (Garaba and Bonthond, 2022b) and rbcL genes (Garaba and Bonthond, 2022a) (under accession number OP925098). Very strong similarities (> 99 %) to *N. spumigena* sequences were obtained from the Basic Local Alignment Search Tool (BLAST) searches against the National Center for Biotechnology Information (NCBI) nucleotide collection. Both genes had 100 % matches with homologues from the strain *N. spumigena* UHCC 0039, of which the genome is available. When we limited the search to type strains only, the type strain of *N. spumigena* (PCC 73104; Lehtimäki et al., 2000) was identified as the best match, with 98.93 % and 95.69 % similarity to the 16S rRNA and rbcL genes, respectively.

### 3.3 Hyperspectral characteristics

#### 3.3.1 Absorption measurements

The absorption coefficient spectra measured with the PSICAM for sampling done in August 2021 and 2022 (Fig. 3) showed shapes typical of water samples containing phytoplankton. In fact, it could be seen that the total absorption coefficient spectrum of the water constituents measured was dominated by the phytoplankton pigments, as their absorption peaks were clearly visible and the typical exponential increase towards the shorter wavelengths (Kirk, 2011) caused by coloured dissolved organic material and non-algal particles was less prominent. This is supported by the comparison of the $a_{tot}$ and $a_{cdom}$ measurements (Fig. 3) in 2022: it is noticeable that $a_{cdom}$ is considerably smaller than $a_{tot}$ in most parts of the spectrum. The values of $a_{cdom}$ were nearly uniform in the lake; thus, spatial changes in $a_{tot}$ were driven by particulate/phytoplankton absorption ($a_{ph}$). Generally, $a_{tot}$ and $a_{ph}$ spectra are dominated by two large peaks in the blue $\sim$ 440 nm and in the red $\sim$ 680 nm, attributable to the presence of chlorophyll *a*. Additional absorption peaks were revealed by fourth derivatives of the measured absorption coefficient spectra at $\sim$ 416, 464, 496, 630, 642 and 682 nm (Fig. 3). The peaks from the derivative analysis are related to chlorophyll *a* and the presence of other photosynthetic or photo-protective pigments. The spectral shapes of the collected water samples at the various sampling locations were quite similar, suggesting a general presence of *N. spumigena* in the various areas of Lake Bante. However, a striking difference that was observed was the presence of a peak at 574 nm in the samples considered to be non-bloom or those with a low presence of *N. spumigena*. Furthermore, the peaks around 630 and 642 nm were absent in the derivative analysis of some sample spectra (Fig. 3). One possible benefit of knowing about these absorption features would be the development of simplified algorithms that could be used to optically infer or detect a *Nodularia* bloom, for example, in Lake Bante using an automated continuous in-water absorption sensor.

In remote sensing, a common way of detecting cyanobacterial blooms involves the use of salient spectral features in the measured reflectance or absorption signal caused by the phycobilin pigments unique to the specific phytoplankton group. Four major groups of phycobilins that have different absorption maxima include phycoerythrin (490–575 nm), phycoerythrocyanin (570–595 nm), phycocyanin (615–640 nm) and allophycocyanin (620–655 nm), as proposed in literature (Seppälä et al., 2007; Sidler, 1994; Rowan, 1989). Furthermore, satellite remote sensing of cyanobacteria often utilizes the 620 nm waveband as a proxy for phycocyanin (Stefan et al., 2005; Wang et al., 2016). The Lake Bante bloom sample absorption coefficient signal did not reveal this feature, although peaks were observed in the derivative spectra at shifted neighbouring wavebands (630 and 642 nm). However, this is not necessarily contradictory to the presence of cyanobacteria, as the phycobilin content in these organisms can vary largely depending on the physiological status and environmental conditions, such as irradiation (Seppälä et al., 2007). It has been reported that the photobleaching of phycobilins tends to occur under strong-radiation conditions (Donkor and Häder, 1996). As the samples were taken from the surface, where ultraviolet and visible irradiation is strongest, we believe that this might be related to the absence of peaks in the region of phycocyanin and allophycocyanin. The possible differences in the phycobilin content of cells from various areas of the lake might also be explained by variations in the physiological status of the cells. *Nodularia* blooms usually develop in the upper 5 m and float with age towards the surface, where scum formation occurs (Gröndahl, 2009). Therefore, it is likely that the

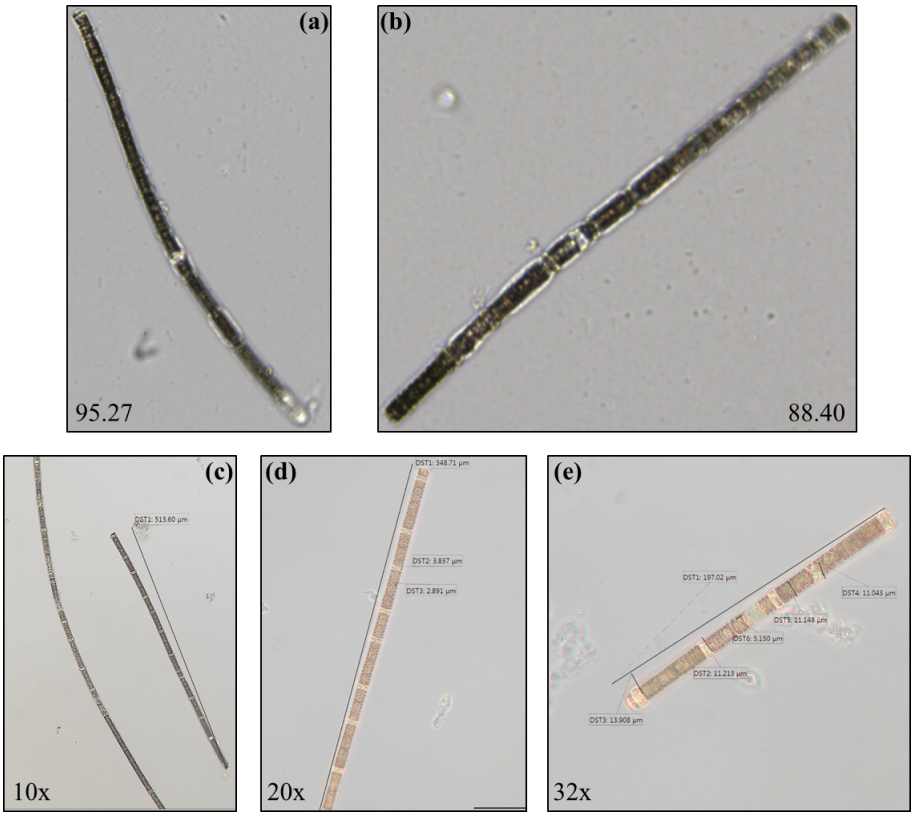


**Figure 2.** **(a–b)** FlowCam images highlighting the area-based diameter (in µm) as a measure of particle size and **(c–e)** JENOPTIK PROGRES® GRYPHAX® KAPELLA microscope photos magnified from 10× to 32× of *N. spumigena* observed during the bloom in Lake Bante on 16 August 2021.

populations of some samples might have had some phycoerythrocyanin, whereas others did not, which could also explain the presence/absence of the observed peak at 574 nm. An alternative explanation, as the peak was absent especially in the very highly concentrated samples, could be strong masking by the proportionally higher absorption in the red part of the spectrum in the bloom sample or suggests the presence of other phytoplankton types in the non-bloom areas. The presence or absence of the peak at 574 nm could be used in a stepwise binary algorithm to eliminate or identify blooms in remote-sensing observations.

### 3.3.2 Fluorescence excitation–emission

Diagnostic peaks were found in the fluorescence signals of the Lake Bante bloom sample, and these signals are characteristic and common for waters with terrestrial sources (Table 1). Three distinct excitation–emission (Ex/Em) regions were revealed in the raw fluorescence spectrum (Fig. 4).

*T* and *B* peaks located at Ex/Em = 275/325 nm indicated the possible presence of autochthonous tryptophan and methionine-like components, also associated with biological activity (Coble, 2007; Kwon et al., 2018). Anthropogenic activities around Lake Bante could contribute to the C peak found at Ex/Em = 350/475 nm, also related to ultraviolet-A (UVA) humic-like compounds of allochthonous origin (Coble, 2007). The lake is surrounded by restaurants, gardens, and residential and industrial structures that might contribute to the production and release of humic-like compounds into the waterbody (Fig. 1). Pigment-like compounds with Ex/Em = 390/620 nm have been reported to be associated with protochlorophyllide species (Remelli and Santabarbara, 2018; Myśliwa-Kurdziel et al., 2003; Campbell et al., 1998). These highly fluorescent precursors are present in cyanobacteria exhibiting signatures that can be detected over an emission range of 620 to 650 nm (Böddi et al., 1998). It is also possible that cyanobacteria distributions can be assessed using phycocyanin-related peaks instead of chlorophyll-*a* in vivo fluorescence located in the non-fluorescing photosystem I. Furthermore, a correlation between the filamentous algal biomass and the intensity of the phycocyanin peak at Ex/Em = 620/650 nm has been proposed as an indicator in remote sensing of algal bloom events (Seppälä et al., 2007).

Example PARAFAC analyses also revealed the presence of four main components, identified as C1, C2, C3 and C4 (Fig. 5, Table 1). Interestingly, the peak located at 390/620 was missing in our analysis due to a limited sensor sensitivity in the red spectrum. In any case, PARAFAC components

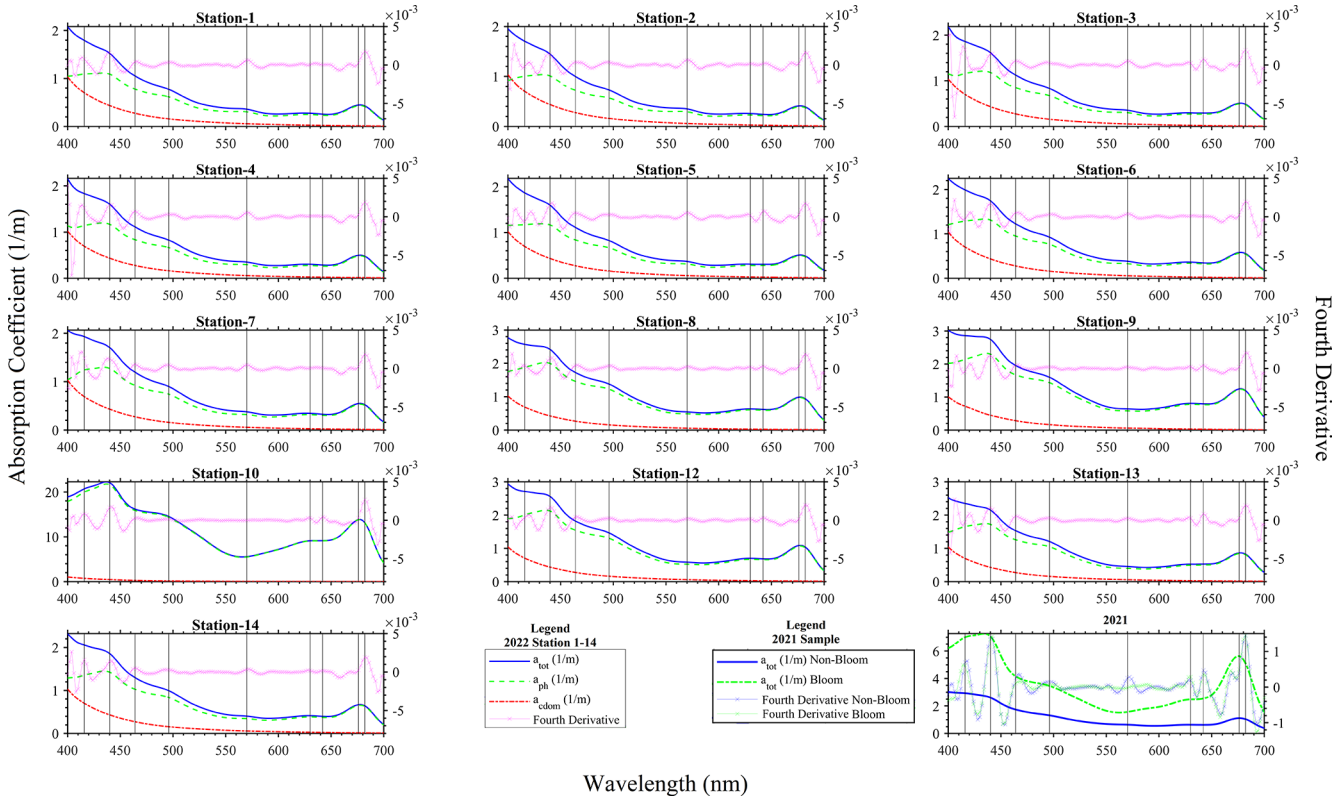


**Figure 3.** Absorption coefficients and fourth-derivative spectra for the 25 August 2022 at stations 1–14 and for the 16 August 2021 sampling of *N. spumigena* bloom events on Lake Bante, Germany. Note that Station 11 is missing from the 2022 campaign.

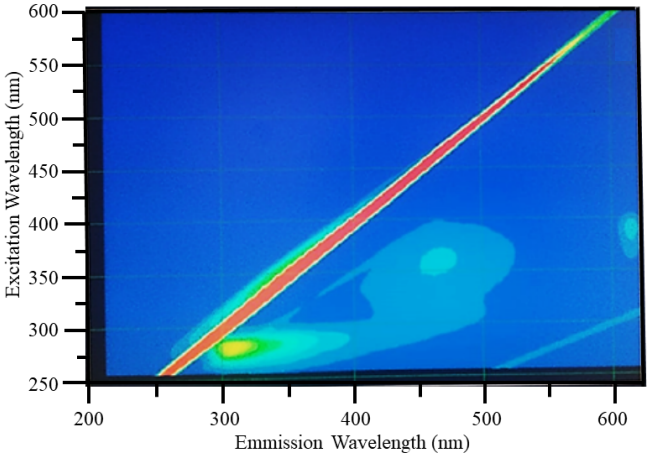


**Figure 4.** Example raw excitation–emission (Ex/Em) fluorescence results: diagnostic Ex/Em peaks located at 275/325, 350/475 and 390/620 nm were observed in the bloom water collected from Lake Bante on 16 August 2021.

derived from our study correspond to well-known chemical groups, namely, tyrosine and tryptophane substances linked to C1 and C2 components as well as humic-A- and humic-C-like substances related to the C3 and C4 components (Hudson et al., 2007).

Fluorescence in our samples was dominated by peaks C1 and C2, commonly referred to as proxies for compounds derived in situ that are indicative of microbiological activity in the investigated waters. The overall composition of the fluorescence spectra shows that up to 30 % of the total fluorescence intensity can be assigned to humic-acid-like compounds ubiquitous in coastal waters (Coble, 1996; Repeta, 2015). Similarly, up to 70 % of the total fluorescence suggests materials derived in situ, namely, tyrosine- and tryptophane-like substances. Enhanced peaks have been associated with the biological reprocessing of DOM in surface waters (Khan et al., 2019). This is consistent with an algal bloom event in which photo-degraded residues of decaying organic matter, e.g. cells, exopolymers, or carbohydrates, are reutilized by microorganisms in surface waters, thereby producing high values for those indicators (Miranda et al., 2018; Lopes et al., 2020; Weiwei et al., 2019).

### 3.3.3 Spectral reflectance

As expected in vegetation or algae, a red-edge feature was observed in the spectral reflectance measured from the bloom water and a peak matching the apparent dark-green

**Table 1.** Example descriptive summary of the PARAFAC components derived from bloom water collected from Lake Bante on 16 August 2021.

| Component | Excitation wavelength (nm) | Emission wavelength (nm) | Literature | Possible origin |
|---|---|---|---|---|
| C1 | 278 | 307 | C3 (Wünsch et al., 2015) | In situ, microbiological |
| C2 | 278 | 348 | C7 (Osburn et al., 2015) | In situ, microbiological |
| C3 | 258/302 | 465 | C2 (Lin and Guo, 2020) | Allochthonous |
| C4 | 250/376 | 488 | C3 (Gao and Guéguen, 2017) | Allochthonous |
| C5* | 390 | 620 | Seppälä et al. (2007) | Protochlorophyllide |

* Component could not be derived in PARAFAC but was observed in the raw data by visual inspection.

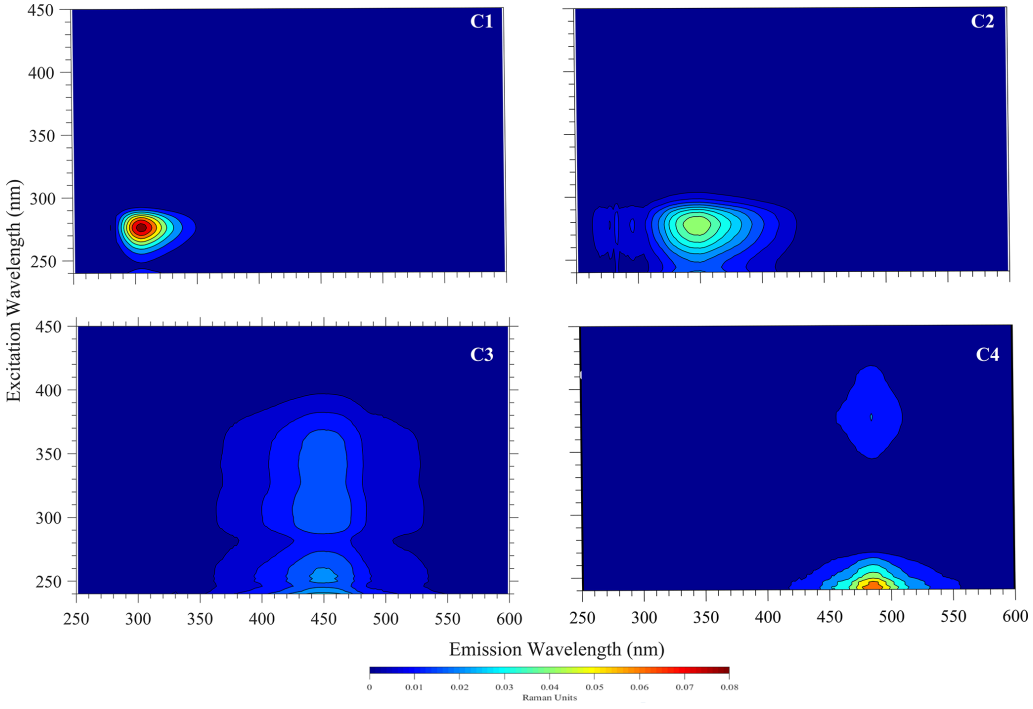


**Figure 5.** Four fluorescent components (C1–C4) derived by the PARAFAC model for the sampled surface water with *N. spumigena* bloom in Lake Bante on 16 August 2021.

(∼ 560 nm) colour of the bloom was also evident in the visible spectrum (Fig. 6). Derivative analysis showed major absorption features at 298, 437, 633, 676, 837, 986 and 1201 nm. Variability in the pseudo-replicate measurements observed could be related to the drift of the boat during field observations. For the 2 years, the laboratory-based 2021 data had the highest magnitude, reaching ∼ 0.6, whereas the in situ 2022 reflectance was ∼ 0.27 in the near-infrared wavebands. Indeed, differences in settings (e.g. density of algae, variable lighting conditions, changes in environment, and light source) in the laboratory and in situ spectral measurements could be sources of some uncertainty in the data.

We also put the measurement that we collected into context by including reported blooms caused by *Ulva prolifera* (Hu et al., 2017), *Tricodesmium* (McKinna et al., 2011) and *N. spumigena* (Soja-Woźniak et al., 2018). A comprehensive quantitative comparison of the spectra was not completed because of the missing metadata in the various studies; for example, some observations were conducted in a laboratory, such as Soja-Woźniak et al. (2018), whereas other observations, such as those undertaken by McKinna et al. (2011), were carried out on research vessels. However, it is evident that all of the spectra share similarities in shape, although they have differences in magnitude (Fig. 7). Therefore, any algorithm based on the measured spectral shape would be appropriate for the detection of such blooms, instead of the magnitude-dependent approach. A red edge is noticeable in all of the spectra, and there is diagnostic peak at around 550 nm. *Ulva prolifera* and *N. spumigena* had nearly the same spectral shape over the measured spectrum; however,

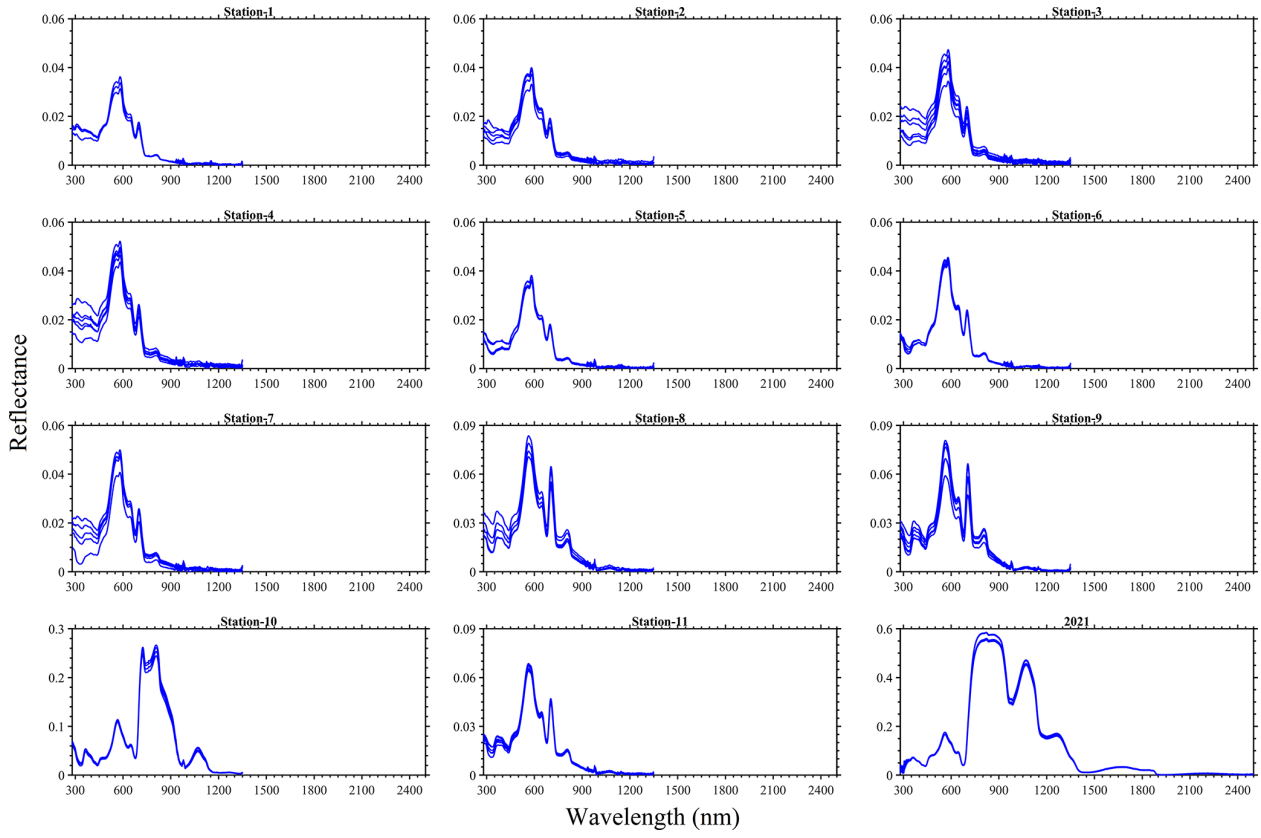


**Figure 6.** Reflectance spectra for the 25 August 2022 at stations 1–11 and for the 16 August 2021 sampling of *N. spumigena* bloom events on Lake Bante, Germany.

the reflectance magnitude was alike up until ∼ 750 nm before differences were noted in the infrared band.

### 3.4 Water quality descriptors

A set of biophysical environmental variables were determined during the 2022 experiment of opportunity. The algal pigments observed were chlorophyll *a* and phycocyanin. The average chlorophyll-*a* concentration was $0.52 \pm 0.37\,\mathrm{mg\,L^{-1}}$, with a range of 0.1–1.45 $\mathrm{mg\,L^{-1}}$. However, phycocyanin levels were highly variable, ranging from 2 to 20.15 $\mu\mathrm{g\,L^{-1}}$ with a mean concentration of $5.14 \pm 5.13\,\mu\mathrm{g\,L^{-1}}$. No direct relationship was found between chlorophyll *a* and phycocyanin. The water clarity inferred from the Secchi disc depth was observed to be indirectly related to the phycocyanin concentration. Overall, water clarity was relatively low ($0.77 \pm 0.23$ m), with the lowest visibility at 0.2 m and the highest visibility at 1 m. Salinity in the lake was generally consistent, with a mean of $10.57 \pm 0.02$ psu and a range between 10.52 to 10.60 psu, suggesting a nearly freshwater environment. The temperature was consistent with the summer season, with the surface water expected to be warm. The mean temperature was $23.01 \pm 0.46$ °C, and the minimum observed was 22.31 °C; the highest measurements (above 23 °C) were around the dense-bloom areas (e.g. stations 9–11).

## 4 Discussion, limitations and recommendations

Bloom events linked to *N. spumigena* have been widely reported across the globe (e.g. Kahru and Elmgren, 2014; Leppänen et al., 1995; Mazur and Pliński, 2003; IOCCG, 2021; Olofsson et al., 2020), but hyperspectral characterization of the optical properties of this cyanobacterium is limited. Therefore, the presented dataset and metadata are expected to contribute to the already available multispectral datasets with the additional benefit of hyperspectral and verified DNA information, especially of the identified bloom caused by *N. spumigena*. Despite the limited number of stations studied during our experiments of opportunity, it is presumed that the gathered high-quality information is a step ahead in advancing scientific-evidence-based knowledge, especially on the potentially toxic *N. spumigena*.

The in situ sampling and data measurement protocols, including error mitigation techniques used during the campaign, were considered to be robust as well as modern. Key steps implemented to mitigate these possible uncertainties included the following: (i) the water containers were pre-rinsed

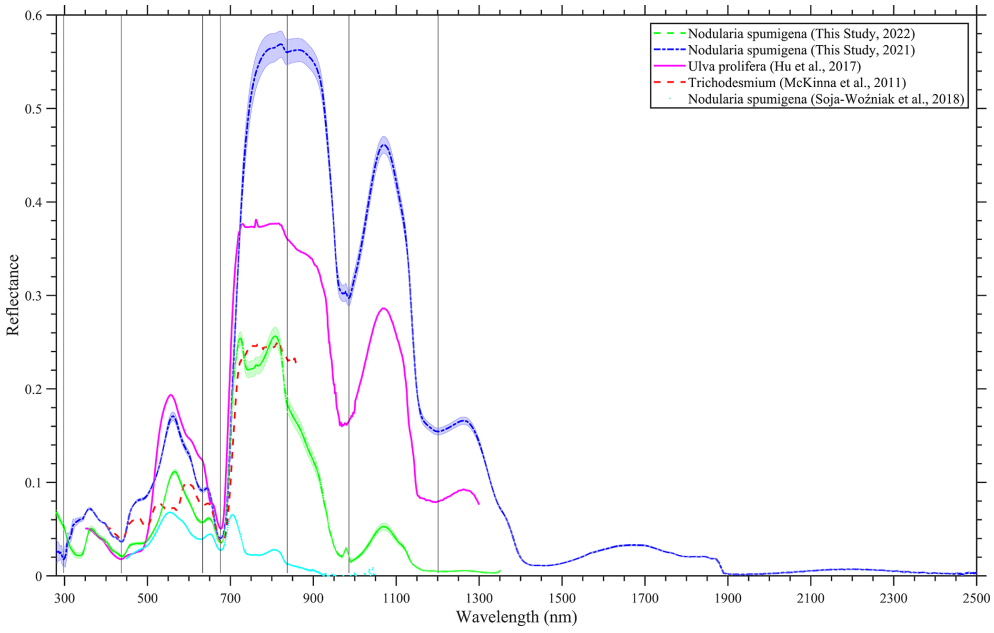


**Figure 7.** A comparison of hyperspectral reflectance spectra of bloom events in Lake Bante, Germany (laboratory-based for 2021 and in situ for 2022); the Yellow Sea (Hu et al., 2017); the Great Barrier Reef (McKinna et al., 2011); and the Baltic Sea (Soja-Woźniak et al., 2018). The Lake Bante spectra are presented as average reflectance, and the shading represents 1 standard deviation.

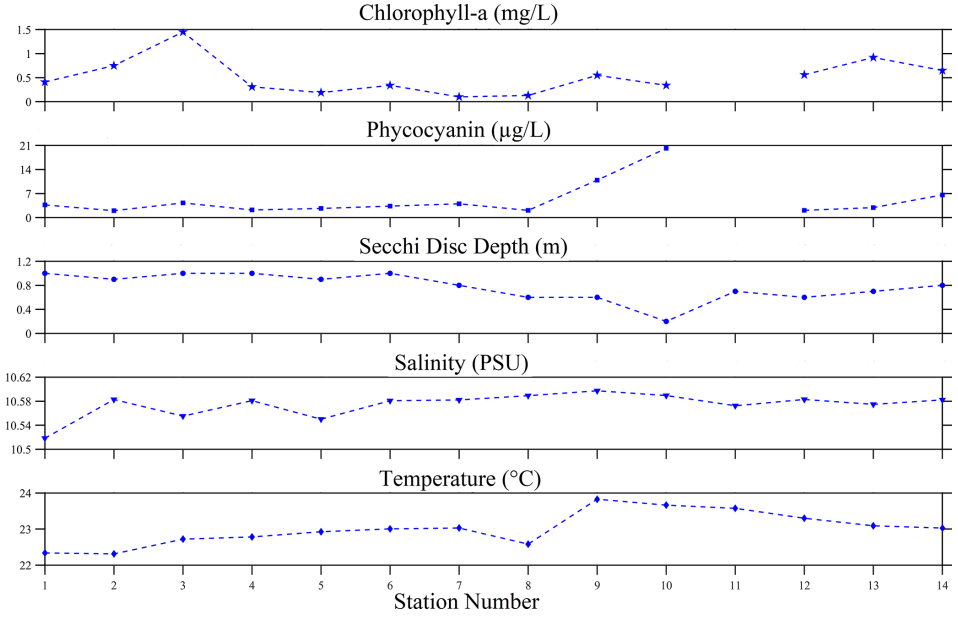


**Figure 8.** Chlorophyll *a*, phycocyanin, Secchi disc depth, salinity and temperature from 25 August 2022 surface water sampling of the *N. spumigena* bloom event on Lake Bante, Germany.

prior to sampling to avoid contamination; (ii) optical observations were an average of 20–30 scans that improved the signal-to-noise ratio, as seen in generated spectra; (iii) modern sampling and analysis protocols were used for the various variables (e.g. radiance, absorbance, absorption, fluorescence, and DNA); and (iv) rigorous visual inspection of spectra and images was carried out. The dynamic nature of the environmental conditions (e.g. wind direction, capillary waves, clouds, and currents) during radiance observations on Lake Bante was challenging to avoid, but effort was made to guarantee the optimal viewing angles in order to reduce possible surface-reflected glint in the observations. In terms of

the absorption measurements, we acknowledge that there is a caveat with respect to our assumption of the dominant constituents being the dissolved and algal material. During the sampling, Lake Bante was relatively calm and most of the surrounding land was either covered by grass, trees, shrubs or paved surfaces (Fig. 1a), suggesting few terrestrial sources, and thus a low concentration, of non-algal suspended material. Although the absorption coefficient of the non-algal suspended material was not measured in this study, it is suggested that this parameter should be considered in future in order to further characterize the optical properties of the waterbody.

It is challenging to identify the algae responsible for blooms without hyperspectral observations and in situ measurements. Thus, we believe that a combination of multi- to hyperspectral tools as well as auxiliary measurements are a prerequisite for developing robust diagnostic algorithms for the potential remote identification of *N. spumigena* after successful detection of the bloom. In this study, we acknowledge that the dataset was constrained; thus, further effort is required to continuously monitor changes in various aquatic environments via social media, local newspapers, regular visual inspection, and in situ hyperspectral measurements with matching satellite imagery. Moreover, all of these in situ measurements ought to undergo through rigorous curation and be made openly accessible.

These recommendations apply to the wide range of bloom-causing species and waterbodies across the globe. Thus, future efforts are encouraged to further establish endmember open-access databases of comparable and traceable hyperspectral measurements that will be accompanied by essential metadata for robust identification as well as detection of HABs from remote sensing. Essential open-access metadata would be observations of parameters such as absorption, scattering coefficients, temperature, salinity, coloured dissolved organic matter, and non-algal and algal particle concentrations to better classify a bloom event. Gathering a whole suite of essential variables has the potential to allow for a comprehensive identification and characterization of a HAB event, and it could also be combined with an optical closure exercise. However, as we inferred from prior related studies (e.g. Dierssen et al., 2015; Seppälä et al., 2007; Kahru et al., 2011), HABs can be challenging to predict. Limitations in the forecasting capabilities of similar blooms restrict in situ measurements to experiments of opportunity, whereby metadata or observations of other essential variables are not always readily available due to constraints related to instrumentation, environmental perturbations, platforms or auxiliary tools.

## 5 Data availability

Curation of the observed data was done following the SeaDataNet recommendations. All of the datasets are openly accessible via the online repositories listed in Table 2.

## 6 Conclusions and outlook

Monitoring of cyanobacteria blooms is of great importance for water quality monitoring, and benchmark information can be derived from satellite remote sensing. Although resolving the phytoplankton functional types responsible for a specific bloom could be limited by the spectral resolution of the satellite sensors, it is feasible to at least detect and map the distributions. In this study, we report hyperspectral properties of *N. spumigena* from an event that can be considered a HAB. Thus, our high-quality in situ dataset is expected to contribute to algorithm development and potential operational monitoring of similar blooms from current or planned hyperspectral satellite missions such as those of the German Aerospace Center (Environmental Mapping and Analysis Program – EnMAP), the Japan Aerospace Exploration Agency (Hyperspectral Imager Suite – HISUI), the National Aeronautics and Space Administration (Plankton, Aerosol, Cloud, ocean Ecosystem – PACE), or the Italian Space Agency (Hyperspectral Precursor of the Application Mission – PRISMA). The current dataset has a unique geographic location, timescale and satellite overpass match-up window ($\sim 2$ h) as well as hyperspectral measurements that can be considered an addition to related datasets, such as the updated European Space Agency (ESA) Ocean Colour Climate Change Initiative (Valente et al., 2022) and the National Aeronautics and Space Administration Hyperspectral Imager for the Coastal Ocean reflectance of floating matters (Hu, 2022), or Belgian lake water quality properties (Castagna et al., 2022).

The application of the phycocyanin peaks in the fluorescence spectrum associated with the presence of cyanobacteria should be explored in the context of the ESA FLEX mission. By utilizing the diagnostic fluorescence signal, HAB detection and identification could be improved, especially when other satellite missions are used in synergy to fuse hyperspectral and high-geospatial-resolution imagery. Reference measurements would need to combine online surveillance systems with physicochemical parameters providing HAB descriptor conditions, such as nitrogen concentration, the intensity of ultraviolet radiation and temperature. It is important to consider the combined use of local knowledge, nowcasting water quality and forecasting of bloom events to potentially focus dedicated interdisciplinary experiments to gather essential as well as comprehensive auxiliary measurements that otherwise tend to be lacking in experiments of opportunity.

**Table 2.** Description of data availability and references for the measurements related to the *N. spumigena* bloom in Lake Bante.

| Description | DOI | Reference |
|---|---|---|
| Absorbance and fluorescence measurements, 2021 | https://doi.org/10.4121/21904632.v1 | Miranda and Garaba (2023) |
| Absorbance and fluorescence measurements, 2022 | https://doi.org/10.4121/21822051.v1 | Miranda et al. (2023) |
| Absorption coefficient measurements, 2021–2022 | https://doi.org/10.4121/21610995.v1 | Wollschläger et al. (2022) |
| Chlorophyll-*a* and phycocyanin concentrations, 2022 | https://doi.org/10.4121/21792665.v1 | Rohde et al. (2023) |
| rbcL genes, 2022 | https://www.ncbi.nlm.nih.gov/nuccore/OP925098 (last access: 15 September 2023) | Garaba and Bonthond (2022a) |
| 16S rRNA, 2022 | https://www.ncbi.nlm.nih.gov/nuccore/OP918142 (last access: 15 September 2023) | Garaba and Bonthond (2022b) |
| Radiance measurements and manufacturer calibration reflectance of the diffuse white standard panel, 2022 | https://doi.org/10.4121/21814773.v1 | Garaba and Albinus (2023) |
| Reflectance from laboratory-based measurements, 2021 | https://doi.org/10.4121/21814977.v1 | Garaba (2023) |
| Secchi disc measurements | https://doi.org/10.1594/PANGAEA.951239 | Garaba and Albinus (2022) |

**Author contributions.** SPG conceived the experiments of opportunity and prepared the text with input from all co-authors. MA, GB, SF, MLMM, SR, JYLY and JW conducted the laboratory analyses of the samples. MA supported the field campaign. All authors reviewed the text.

**Competing interests.** The contact author has declared that none of the authors has any competing interests.

**Disclaimer.** Publisher's note: Copernicus Publications remains neutral with regard to jurisdictional claims in published maps and institutional affiliations.

**Acknowledgements.** We are grateful to Ulrike Graalmann at the City of Wilhelmshaven, Germany, for assisting with permits to conduct research on Lake Bante. Gerrit Behrens, Lutz ter Hell, Helmo Nicolai, Waldemar Siewert and Claudia Thölen helped with the preparation and orchestration of the field campaign.

**Financial support.** Shungudzemwoyo P. Garaba was supported by the Deutsche Forschungsgemeinschaft (grant no. 417276871) and the Discovery Element of the ESA Basic Activities (contract no. 4000132037/20/NL/GLC). PlanetScope imagery was made available through the ESA Third Party Missions programme (project no. 62280). Mario L. M. Miranda was funded by the University of Panama through the Young Professors Grant (grant no. VIP-01-04-16-2018-08) from the Vice Rectorate for Research and Postgraduate Studies (VIP) and the National System of Research (SNI) of the National secretary of Science and Technology (SENACYT).

**Review statement.** This paper was edited by Giuseppe M. R. Manzella and reviewed by two anonymous referees.

## References

Böddi, B., Kis-Petik, K., Kaposi, A. D., Fidy, J., and Sundqvist, C.: The two spectroscopically different short wavelength protochlorophyllide forms in pea epicotyls are both monomeric, Biochim. Biophys. Acta Bioenerg., 1365, 531–540, https://doi.org/10.1016/S0005-2728(98)00106-6, 1998.

Bracher, A., Bouman, H. A., Brewin, R. J. W., Bricaud, A., Brotas, V., Ciotti, A. M., Clementson, L., Devred, E., Di Cicco, A., Dutkiewicz, S., Hardman-Mountford, N. J., Hickman, A. E., Hieronymi, M., Hirata, T., Losa, S. N., Mouw, C. B., Organelli, E., Raitsos, D. E., Uitz, J., Vogt, M., and Wolanin, A.: Obtaining phytoplankton diversity from ocean color: A scientific roadmap for future development, Front. Mar. Sci., 4, 55, https://doi.org/10.3389/fmars.2017.00055, 2017.

Campbell, D., Hurry, V., Clarke, A. K., Gustafsson, P., and Öquist, G.: Chlorophyll fluorescence analysis of cyanobacterial photosynthesis and acclimation, Microbiol. Mol. Biol. Rev., 62, 667–683, https://doi.org/10.1128/MMBR.62.3.667-683.1998, 1998.

Carmichael, W. W.: Cyanobacteria secondary metabolites—the cyanotoxins, J. Appl. Bacteriol., 72, 445–459, https://doi.org/10.1111/j.1365-2672.1992.tb01858.x, 1992.

Castagna, A., Amadei Martínez, L., Bogorad, M., Daveloose, I., Dasseville, R., Dierssen, H. M., Beck, M., Mortelmans, J., Lavigne, H., Dogliotti, A., Doxaran, D., Ruddick, K., Vyverman, W., and Sabbe, K.: Optical and biogeochemical properties of diverse Belgian inland and coastal waters, Earth Syst. Sci. Data, 14, 2697–2719, https://doi.org/10.5194/essd-14-2697-2022, 2022.

Chapra, S. C., Boehlert, B., Fant, C., Bierman, V. J., Henderson, J., Mills, D., Mas, D. M. L., Rennels, L., Jantarasami, L., Martinich, J., Strzepek, K. M., and Paerl, H. W.: Climate change impacts on harmful algal blooms in U.S. freshwaters: A screening-level assessment, Environ. Sci. Technol., 51, 8933–8943, https://doi.org/10.1021/acs.est.7b01498, 2017.

Coble, P. G.: Characterization of marine and terrestrial DOM in seawater using excitation-emission matrix spectroscopy, Mar. Chem., 51, 325–346, https://doi.org/10.1016/0304-4203(95)00062-3, 1996.

Coble, P. G.: Marine optical biogeochemistry: The chemistry of ocean color, Chem. Rev., 107, 402–418, https://doi.org/10.1021/cr050350+, 2007.

da Silveira, S. B., Wasielesky, W., Andreote, A. P. D., Fiore, M. F., and Odebrecht, C.: Morphology, phylogeny, growth rate and nodularin production of Nodularia spumigena from Brazil, Mar. Biol. Res., 13, 1095–1107, https://doi.org/10.1080/17451000.2017.1336587, 2017.

Dierssen, H., McManus, G. B., Chlus, A., Qiu, D., Gao, B.-C., and Lin, S.: Space station image captures a red tide ciliate bloom at high spectral and spatial resolution, P. Natl. Acad. Sci. USA, 112, 14783–14787, https://doi.org/10.1073/pnas.1512538112, 2015.

Donkor, V. A. and Häder, D. P.: Effects of ultraviolet irradiation on photosynthetic pigments in some filamentous cyanobacteria, Aquat. Microb. Ecol., 11, 143–149, https://doi.org/10.3354/ame011143, 1996.

Francis, G.: Poisonous Australian Lake, Nature, 18, 11–12, https://doi.org/10.1038/018011d0, 1878.

Galat, D. L., Verdin, J. P., and Sims, L. L.: Large-scale patterns of Nodularia spumigena blooms in Pyramid Lake, Nevada, determined from Landsat imagery: 1972–1986, Hydrobiologia, 197, 147–164, https://doi.org/10.1007/BF00026947, 1990.

Gao, Z. and Guéguen, C.: Size distribution of absorbing and fluorescing DOM in Beaufort Sea, Canada Basin, Deep-Sea Res. Pt. I, 121, 30–37, https://doi.org/10.1016/j.dsr.2016.12.014, 2017.

Garaba, S. and Bonthond, G.: Uncultured Nodularia sp. clone Banta_env18 ribulose 1,5-biphosphate carboxylase large subunit (rbcL) gene, partial cds; chaperonin-like protein (rbcX) gene, complete cds; and ribulose 1,5-bisphosphate carboxylase small subunit (rbcS) gene, partial cds, GenBank® nucleic acid sequence database [data set], https://www.ncbi.nlm.nih.gov, https://www.ncbi.nlm.nih.gov/nuccore/OP925098 (last access: 15 September 2023), 2022a.

Garaba, S. and Bonthond, G.: Nodularia spumigena 16S rRNA gene, environmental sample Lake Bante. Uncultured Nodularia sp. clone 1 16S ribosomal RNA gene, partial sequence, GenBank® nucleic acid sequence database [data set], https://www.ncbi.nlm.nih.gov, https://www.ncbi.nlm.nih.gov/nuccore/OP918142 (last access: 15 September 2023), 2022b.

Garaba, S. P.: Spectral reflectance measurements of water sample from a Nodularia spumigena bloom event on Lake Bante in Wilhelmshaven, Germany, 4TU.ResearchData Dataset. Avaialable on-line [https://researchdata.4tu.nl/], https://doi.org/10.4121/21814977.v1, 2023.

Garaba, S. P. and Albinus, M.: Secchi disk measurements during Nodularia spumigena bloom on Lake Bante in Wilhemshaven, Germany, PANGAEA [data set], https://doi.org/10.1594/PANGAEA.951239, 2022.

Garaba, S. P. and Albinus, M.: Spectral radiance measurements during a Nodularia spumigena bloom event on Lake Bante in Wilhelmshaven, Germany, 4TU.ResearchData [Data set], https://doi.org/10.4121/21814773.v1, 2023.

Garaba, S. P. and Dierssen, H. M.: Hyperspectral ultraviolet to shortwave infrared characteristics of marine-harvested, washed-ashore and virgin plastics, Earth Syst. Sci. Data, 12, 77–86, https://doi.org/10.5194/essd-12-77-2020, 2020.

Garaba, S. P. and Zielinski, O.: Methods in reducing surface reflected glint for shipborne above-water remote sensing, J. Eur. Opt. Soc.-Rapid, 8, 13058, https://doi.org/10.2971/jeos.2013.13058, 2013.

Garaba, S. P., Arias, M., Corradi, P., Harmel, T., de Vries, R., and Lebreton, L.: Concentration, anisotropic and apparent colour effects on optical reflectance properties of virgin and ocean-harvested plastics, J. Hazard. Mater., 406, 124290, https://doi.org/10.1016/j.jhazmat.2020.124290, 2021.

Glibert, P. M., Anderson, D. M., Gentien, P., Graneli, E., and Sellner, K. G.: The global complex phenomena of harmful algal blooms, Oceanography, 18, 136–147, 2005.

Gröndahl, F.: Removal of surface blooms of the cyanobacteria Nodularia spumigena: A pilot project conducted in the Baltic Sea, AMBIO, 38, 79–84, 2009.

Guiry, M. D. and Guiry, G. M.: AlgaeBase, World-wide electronic publication, https://www.algaebase.org (last access: 15 September 2023), 2021.

Hallegraeff, G. M., Anderson, D. M., and Cembella, A. D.: Manual on harmful marine microalgae, in: Monographs on oceanographic methodology 11, UNESCO Publishing, France, ISBN 92-3-103871-0, https://unesdoc.unesco.org/ark:/48223/pf0000131711 (last access: 15 September 2023), 2003.

Horstmann, U.: Eutrophication and mass production of blue-green algae in the Baltic, Merentutkimuslait. Julk. Havsforskningsinst. Skr., 239 pp., 83–90, 1975.

Horváth, H., Kovács, A. W., Riddick, C., and Présing, M.: Extraction methods for phycocyanin determination in freshwater filamentous cyanobacteria and their application in a shallow lake, Eur. J. Phycol., 48, 278–286, https://doi.org/10.1080/09670262.2013.821525, 2013.

Hu, C.: Hyperspectral reflectance spectra of floating matters derived from Hyperspectral Imager for the Coastal Ocean (HICO) observations, Earth Syst. Sci. Data, 14, 1183–1192, https://doi.org/10.5194/essd-14-1183-2022, 2022.

Hu, C., Qi, L., Xie, Y., Zhang, S., and Barnes, B. B.: Spectral characteristics of sea snot reflectance observed from satellites: Implications for remote sensing of marine debris, Remote Sens. Environ., 269, 112842, https://doi.org/10.1016/j.rse.2021.112842, 2022.

Hu, L., Hu, C., and Ming-Xia, H. E.: Remote estimation of biomass of Ulva prolifera macroalgae in the Yellow Sea, Remote Sens. Environ., 192, 217–227, https://doi.org/10.1016/j.rse.2017.01.037, 2017.

Hudson, N., Baker, A., and Reynolds, D.: Fluorescence analysis of dissolved organic matter in natural, waste and polluted waters – a review, River Res. Appl., 23, 631–649, https://doi.org/10.1002/rra.1005, 2007.

IOCCG: Observation of harmful algal blooms with ocean colour radiometry, Reports of the International Ocean Colour Coordinating Group, No. 20, edited by: Bernard, S., Kudela, R., Robertson Lain, L., and Pitcher, G. C., Dartmouth, Canada, 165 pp., https://doi.org/10.25607/OBP-1042, 2021.

Kahru, M., Horstmann, U., and Rud, O.: Satellite detection of increased cyanobacterial blooms in Baltic Sea: Natural fluctuation or ecosystem change?, AMBIO, 23, 469–472, 1994.

Kahru, M. and Elmgren, R.: Multidecadal time series of satellite-detected accumulations of cyanobacteria in the Baltic Sea, Biogeosciences, 11, 3619–3633, https://doi.org/10.5194/bg-11-3619-2014, 2014.

Kahru, M., Brotas, V., Manzano-Sarabia, M., and Mitchell, B. G.: Are phytoplankton blooms occurring earlier in the Arctic?, Glob. Change Biol., 17, 1733–1739, https://doi.org/10.1111/j.1365-2486.2010.02312.x, 2011.

Kanoshina, I., Lips, U., and Leppänen, J.-M.: The influence of weather conditions (temperature and wind) on cyanobacterial bloom development in the Gulf of Finland (Baltic Sea), Harmful Algae, 2, 29–41, https://doi.org/10.1016/S1568-9883(02)00085-9, 2003.

Karlberg, M. and Wulff, A.: Impact of temperature and species interaction on filamentous cyanobacteria may be more important than salinity and increased $pCO_2$ levels, Mar. Biol., 160, 2063–2072, https://doi.org/10.1007/s00227-012-2078-3, 2013.

Karlson, B., Andersen, P., Arneborg, L., Cembella, A., Eikrem, W., John, U., West, J. J., Klemm, K., Kobos, J., Lehtinen, S., Lundholm, N., Mazur-Marzec, H., Naustvoll, L., Poelman, M., Provoost, P., De Rijcke, M., and Suikkanen, S.: Harmful algal blooms and their effects in coastal seas of Northern Europe, Harmful Algae, 102, 101989, https://doi.org/10.1016/j.hal.2021.101989, 2021.

Karlsson, K. M., Kankaanpää, H. T., Huttunen, M., and Meriluoto, J.: First observation of microcystin-LR in pelagic cyanobacterial blooms in the northern Baltic Sea, Harmful Algae, 4, 163–166, https://doi.org/10.1016/j.hal.2004.02.002, 2005.

Khan, S. I., Zamyadi, A., Rao, N. R. H., Li, X., Stuetz, R. M., and Henderson, R. K.: Fluorescence spectroscopic characterisation of algal organic matter: towards improved in situ fluorometer development, Environ. Sci. Water Res. Technol., 5, 417–432, https://doi.org/10.1039/C8EW00731D, 2019.

Kirk, J. T. O.: Point-source integrating-cavity absorption meter: theoretical principles and numerical modeling, Appl. Optics, 36, 6123–6128, https://doi.org/10.1364/AO.36.006123, 1997.

Kirk, J. T. O.: Light and photosynthesis in aquatic ecosystems, Cambridge University Press, Cambridge, United Kingdom, 662 pp., ISBN 978-0-521-15175-7, 2011.

Komárek, J.: Cyanoprokaryota -3. Teil/Part 3: Heterocytous genera, Süßwasserflora von Mitteleuropa/Freshwater Flora of Central Europe, 19/3, edited by: Büdel, B., Gärtner, G., Krienitz, L., and Schagerl, M., Springer Spektrum, Heidelberg, Germany, XVIII, 1131 pp., ISBN 978-3-8274-0932-4, 2013.

Kwon, H. K., Kim, G., Lim, W. A., and Park, J. W.: In-situ production of humic-like fluorescent dissolved organic matter during Cochlodinium polykrikoides blooms, Estuar. Coast. Shelf S., 203, 119–126, https://doi.org/10.1016/j.ecss.2018.02.013, 2018.

Lehtimaki, J., Moisander, P., Sivonen, K., and Kononen, K.: Growth, nitrogen fixation, and nodularin production by two baltic sea cyanobacteria, Appl. Environ. Microbiol., 63, 1647–1656, https://doi.org/10.1128/aem.63.5.1647-1656.1997, 1997.

Lehtimäki, J., Lyra, C., Suomalainen, S., Sundman, P., Rouhiainen, L., Paulin, L., Salkinoja-Salonen, M., and Sivonen, K.: Characterization of Nodularia strains, cyanobacteria from brackish waters, by genotypic and phenotypic methods, Int. J. Syst. Evol., 50, 1043–1053, https://doi.org/10.1099/00207713-50-3-1043, 2000.

Leppänen, J.-M., Rantajärvi, E., Hällfors, S., Kruskopf, M., and Laine, V.: Unattended monitoring of potentially toxic phytoplankton species in the Baltic Sea in 1993, J. Plankton Res., 17, 891–902, https://doi.org/10.1093/plankt/17.4.891, 1995.

Lin, H. and Guo, L.: Variations in colloidal DOM composition with molecular weight within individual water samples as characterized by flow field-flow fractionation and EEM-PARAFAC analysis, Environ. Sci. Technol., 54, 1657–1667, https://doi.org/10.1021/acs.est.9b07123, 2020.

Liutkus, A.: Scale-space peak picking: Inria, Speech Processing Team, Inria Nancy – Grand Est, Villers-lès-Nancy, France, https://hal.inria.fr/hal-01103123 (last access: 15 September 2023), 2015.

Lopes, R., Miranda, M. L., Schütte, H., Gassmann, S., and Zielinski, O.: Microfluidic approach for controlled ultraviolet treatment of colored and fluorescent dissolved organic matter, Spectrochim. Acta, 239, 118435, https://doi.org/10.1016/j.saa.2020.118435, 2020.

Mazur, H. and Pliński, M.: Nodularia spumigena blooms and the occurrence of hepatotoxin in the Gulf of Gdańsk, Oceanologia, 45, 305–316, 2003.

McKinna, L. I. W., Furnas, M. J., and Ridd, P. V.: A simple, binary classification algorithm for the detection of Trichodesmium spp. within the Great Barrier Reef using MODIS imagery, Limnol. Oceanogr. Meth., 9, 50–66, https://doi.org/10.4319/lom.2011.9.50, 2011.

Miranda, M. L., Mustaffa, N. I. H., Robinson, T. B., Stolle, C., Ribas-Ribas, M., Wurl, O., and Zielinski, O.: Influence of solar radiation on biogeochemical parameters and fluorescent dissolved organic matter (FDOM) in the sea surface microlayer of the southern coastal North Sea, Elem. Sci. Anth., 6, 15, https://doi.org/10.1525/elementa.278, 2018.

Miranda, M. L., Osterholz, H., Giebel, H. A., Bruhnke, P., Dittmar, T., and Zielinski, O.: Impact of UV radiation on DOM transformation on molecular level using FT-ICR-MS and PARAFAC, Spectrochim. Acta, 230, 118027, https://doi.org/10.1016/j.saa.2020.118027, 2020.

Miranda, M. L. M. and Garaba, S. P.: Raw absorbance and fluorescence measurements of water samples during Nodularia spumigena 2021 bloom event on Lake Bante in Wilhelmshaven, Germany, 4TU.ResearchData [data set], https://doi.org/10.4121/21904632.v1, 2023.

Miranda, M. L. M., Albinus, M., and Garaba, S. P.: Raw absorbance and fluorescence measurements of water samples during Nodularia spumigena bloom event on Lake Bante in Wilhelmshaven, Germany, 4TU.ResearchData [data set], https://doi.org/10.4121/21822051.v1, 2023.

Murphy, K. R., Stedmon, C. A., Graeber, D., and Bro, R.: Fluorescence spectroscopy and multi-way techniques, PARAFAC, Anal. Methods-UK, 5, 6557–6566, https://doi.org/10.1039/C3AY41160E, 2013.

Murphy, K. R., Stedmon, C. A., Wenig, P., and Bro, R.: OpenFluor – an online spectral library of auto-fluorescence by organic compounds in the environment, Anal. Methods-UK, 6, 658-661, https://doi.org/10.1039/C3AY41935E, 2014.

Myśliwa-Kurdziel, B., Amirjani, M. R., Strzałka, K., and Sundqvist, C.: Fluorescence lifetimes of protochlorophyllide in plants with different proportions of short-wavelength and long-wavelength protochlorophyllide spectral forms, Photochem. Photobiol., 78, 205–212, https://doi.org/10.1562/0031-8655(2003)0780205FLOPIP2.0.CO2, 2003.

Nehring, S.: Mortality of dogs associated with a mass development of Nodularia spumigena (Cyanophyceae) in a brackish lake at the German North Sea coast, J. Plankton Res., 15, 867–872, https://doi.org/10.1093/plankt/15.7.867, 1993.

Olofsson, M., Suikkanen, S., Kobos, J., Wasmund, N., and Karlson, B.: Basin-specific changes in filamentous cyanobacteria community composition across four decades in the Baltic Sea, Harmful Algae, 91, 101685, https://doi.org/10.1016/j.hal.2019.101685, 2020.

Osburn, C. L., Mikan, M. P., Etheridge, J. R., Burchell, M. R., and Birgand, F.: Seasonal variation in the quality of dissolved and particulate organic matter exchanged between a salt marsh and its adjacent estuary, J. Geophys. Res.-Biogeo., 120, 1430–1449, https://doi.org/10.1002/2014JG002897, 2015.

Öström, B.: Fertilization of the Baltic by nitrogen fixation in the blue-green alga Nodularia Spumigena, Remote Sens. Environ., 4, 305–310, https://doi.org/10.1016/0034-4257(75)90026-7, 1976.

Remelli, W. and Santabarbara, S.: Excitation and emission wavelength dependence of fluorescence spectra in whole cells of the cyanobacterium Synechocystis sp. PPC6803: Influence on the estimation of Photosystem II maximal quantum efficiency, Biochim. Biophys. Acta, 1859, 1207–1222, https://doi.org/10.1016/j.bbabio.2018.09.366, 2018.

Repeta, D. J.: Chapter 2 – Chemical characterization and cycling of dissolved organic matter, in: Biogeochemistry of marine dissolved organic matter, 2nd Edn., edited by: Hansell, D. A. and Carlson, C. A., Academic Press, Boston, USA, 21–63, https://doi.org/10.1016/B978-0-12-405940-5.00002-9, 2015.

Ritchie, R. J.: Universal chlorophyll equations for estimating chlorophylls $a, b, c,$ and $d$ and total chlorophylls in natural assemblages of photosynthetic organisms using acetone, methanol, or ethanol solvents, Photosynthetica, 46, 115–126, https://doi.org/10.1007/s11099-008-0019-7, 2008.

Rohde, S., Albinus, M., and Garaba, S. P.: Chlorophyll-a and phycocyanin concentrations from a Nodularia spumigena bloom event on Lake Bante in Wilhelmshaven, Germany, 4TU.ResearchData [data set], https://doi.org/10.4121/21792665.v1, 2023.

Röttgers, R. and Doerffer, R.: Measurements of optical absorption by chromophoric dissolved organic matter using a point-source integrating-cavity absorption meter, Limnol. Oceanogr. Meth., 5, 126–135, https://doi.org/10.4319/lom.2007.5.126, 2007.

Rowan, K. S.: Photosynthetic pigments of algae, Cambridge University Press, United States of America, xiii, 334, ill. pp., ISBN 0521301769, 1989.

Seppälä, J., Ylöstalo, P., Kaitala, S., Hällfors, S., Raateoja, M., and Maunula, P.: Ship-of-opportunity based phycocyanin fluorescence monitoring of the filamentous cyanobacteria bloom dynamics in the Baltic Sea, Estuar. Coast. Shelf S., 73, 489–500, https://doi.org/10.1016/j.ecss.2007.02.015, 2007.

Sidler, W. A.: Phycobilisome and phycobiliprotein structures, in: The molecular biology of cyanobacteria, edited by: Bryant, D. A., Springer Netherlands, Dordrecht, 139–216, https://doi.org/10.1007/978-94-011-0227-8_7, 1994.

Sivonen, K., Kononen, K., Carmichael, W. W., Dahlem, A. M., Rinehart, K. L., Kiviranta, J., and Niemela, S. I.: Occurrence of the hepatotoxic cyanobacterium Nodularia spumigena in the Baltic Sea and structure of the toxin, Appl. Environ. Microbiol., 55, 1990–1995, https://doi.org/10.1128/aem.55.8.1990-1995.1989, 1989.

Smayda, T. J.: Harmful algal blooms: Their ecophysiology and general relevance to phytoplankton blooms in the sea, Limnol. Oceanogr., 42, 1137–1153, https://doi.org/10.4319/lo.1997.42.5_part_2.1137, 1997.

Soja-Woźniak, M., Darecki, M., Wojtasiewicz, B., and Bradtke, K.: Laboratory measurements of remote sensing reflectance of selected phytoplankton species from the Baltic Sea, Oceanologia, 60, 86–96, https://doi.org/10.1016/j.oceano.2017.08.001, 2018.

Stefan, G. H. S., Steef, W. M. P., and Gons, H. J.: Remote sensing of the cyanobacterial pigment phycocyanin in turbid inland water, Limnol. Oceanogr., 50, 237–245, https://doi.org/10.4319/lo.2005.50.1.0237, 2005.

Teikari, J. E., Fewer, D. P., Shrestha, R., Hou, S., Leikoski, N., Mäkelä, M., Simojoki, A., Hess, W. R., and Sivonen, K.: Strains of the toxic and bloom-forming Nodularia spumigena (cyanobacteria) can degrade methylphosphonate and release methane, ISME J., 12, 1619–1630, https://doi.org/10.1038/s41396-018-0056-6, 2018.

Utermöhl, H.: Neue Wege in der quantitativen Erfassung des Plankton. (Mit besonderer Berücksichtigung des Ultraplanktons.), SIL Proceedings, 1922–2010, Internationale Vereinigung für Theoretische und Angewandte Limnologie: Verhandlungen, 5, 567–596, https://doi.org/10.1080/03680770.1931.11898492, 1931.

Valente, A., Sathyendranath, S., Brotas, V., Groom, S., Grant, M., Jackson, T., Chuprin, A., Taberner, M., Airs, R., Antoine, D., Arnone, R., Balch, W. M., Barker, K., Barlow, R., Bélanger, S., Berthon, J.-F., Beşiktepe, Ş., Borsheim, Y., Bracher, A., Brando, V., Brewin, R. J. W., Canuti, E., Chavez, F. P., Cianca, A., Claustre, H., Clementson, L., Crout, R., Ferreira, A., Freeman, S., Frouin, R., García-Soto, C., Gibb, S. W., Goericke, R., Gould, R., Guillocheau, N., Hooker, S. B., Hu, C., Kahru, M., Kampel, M., Klein, H., Kratzer, S., Kudela, R., Ledesma, J., Lohrenz, S., Loisel, H., Mannino, A., Martinez-Vicente, V., Matrai, P., McKee, D., Mitchell, B. G., Moisan, T., Montes, E., Muller-Karger, F., Neeley, A., Novak, M., O'Dowd, L., Ondrusek, M., Platt, T., Poulton, A. J., Repecaud, M., Röttgers, R., Schroeder, T., Smyth, T., Smythe-Wright, D., Sosik, H. M., Thomas, C., Thomas, R., Tilstone, G., Tracana, A., Twardowski, M., Vellucci, V., Voss, K., Werdell, J., Wernand, M., Wojtasiewicz, B., Wright, S., and Zibordi, G.: A compilation of global bio-optical in situ data for ocean colour satellite applications – version three, Earth Syst. Sci. Data, 14, 5737–5770, https://doi.org/10.5194/essd-14-5737-2022, 2022.

Wang, G., Lee, Z., Mishra, D. R., and Ma, R.: Retrieving absorption coefficients of multiple phytoplankton pigments from hyperspectral remote sensing reflectance measured over cyanobacteria bloom waters, Limnol. Oceanogr. Meth., 14, 432–447, https://doi.org/10.1002/lom3.10102, 2016.

Wasmund, N.: Occurrence of cyanobacterial blooms in the baltic sea in relation to environmental conditions, Int. Revue ges. Hydrobiol., 82, 169–184, https://doi.org/10.1002/iroh.19970820205, 1997.

Weiwei, L., Xin, Y., Keqiang, S., Baohua, Z., and Guang, G.: Unraveling the sources and fluorescence compositions of dissolved and particulate organic matter (DOM and POM) in Lake Taihu, China, Environ. Sci. Pollut. Res., 26, 4027–4040, https://doi.org/10.1007/s11356-018-3873-2, 2019.

Wollschläger, J., Albinus, M., and Garaba, S. P.: Absorption measurements of Nodularia spumigena bloom from Lake Bante in Wilhelmshaven, Germany, 4TU.ResearchData [data set], https://doi.org/10.4121/21610995.v1, 2022.

Wünsch, U. J., Murphy, K. R., and Stedmon, C. A.: Fluorescence quantum yields of natural organic matter and organic compounds: Implications for the fluorescence-based interpretation of organic matter composition, Front. Mar. Sci., 2, 98, https://doi.org/10.3389/fmars.2015.00098, 2015.